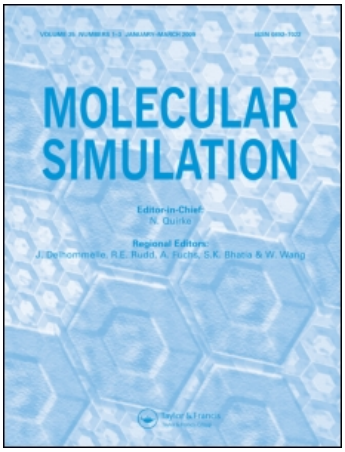

Molecular Simulation
Publication details, including instructions for authors and subscription information:
http://www.informaworld.com/smpp/title~content=t713644482

Ad hoc continuum-atomistic thermostat for modeling heat flow in molecular dynamics simulations

J. David Schall[a]; Clifford W. Padgett[a]; Donald W. Brenner[a]
[a] Department of Materials Science and Engineering, North Carolina State University, Raleigh, NC, USA

To cite this Article Schall, J. David , Padgett, Clifford W. and Brenner, Donald W.(2005) '*Ad hoc* continuum-atomistic thermostat for modeling heat flow in molecular dynamics simulations', Molecular Simulation, 31: 4, 283 — 288
To link to this Article: DOI: 10.1080/08927020512331336898
URL: http://dx.doi.org/10.1080/08927020512331336898

Molecular Simulation, Vol. 31, No. 4, 15 April 2005, 283–288

Taylor & Francis
Taylor & Francis Group

Ad hoc continuum-atomistic thermostat for modeling heat flow in molecular dynamics simulations

J. DAVID SCHALL, CLIFFORD W. PADGETT and DONALD W. BRENNER*

Department of Materials Science and Engineering, North Carolina State University, Raleigh, NC 27695-7907, USA

(Received July 2004; in final form December 2004)

An *ad hoc* thermostating procedure that couples a molecular dynamics (MD) simulation and a numerical solution to the continuum heat flow equation is presented. The method allows experimental thermal transport properties to be modeled without explicitly including electronic degrees of freedom in a MD simulation. The method is demonstrated using two examples, heat flow from a constant temperature silver surface into a single crystal bulk, and a tip sliding along a silver surface. For the former it is shown that frictional forces based on the Hoover thermostat applied locally to grid regions of the simulation are needed for effective feedback between the atomistic and continuum equations. For fast tip sliding the thermostat results in less surface heating, and higher frictional and normal forces compared to the same simulation without the thermostat.

Keywords: Molecular dynamics simulation; Molecular heat flow; Continuum-Atomistic Thermostat; Continuum heat flow

1. Introduction

Many different thermostating schemes have been developed for use in molecular dynamics (MD) simulations. The earliest schemes used simple velocity scaling to equilibrate to a given temperature [1]. Starting in the 1970s schemes were introduced in which "reactive regions" were surrounded by thermostated atoms. In methodologies developed by Tully [2], Adelman [3], Doll [4] and others [5–7], for example, a boundary region in which both Langevin forces and forces from an interatomic potential are used is introduced around a reaction region in which only forces from the potential act on the atoms. The boundary region acts as a heat source/sink, and in principle the Langevin forces on the atoms in this region do not significantly alter the dynamics of the reaction region as long as the reaction region is sufficiently large. Langevin forces obtained from detailed memory kernels with properties derived from phonon spectra [2] or forces based on simplified Debye models have been used in the boundary regions [3].

Thermostats have also been developed that utilize constraints and driving forces on the equations of motion [8]. These forces lead to a feedback between the temperature of the system and the forces on the atoms. Using the principle of least constraint, for example, Evans, Hoover and co-workers derived a frictional force with coefficient γ given by

$$\gamma = \left[\frac{-\sum_j \bar{F}_j \cdot \bar{V}_j}{\sum_j V_j^2 m_j}\right] \tag{1}$$

that maintains the total kinetic energy in a simulation [9]. In equation (1) F_j, V_j and m_j are the total force on atom j from the interatomic potential, the velocity of atom j and the mass of atom j, respectively. The sum is typically over all atoms in the simulation, and the frictional force is applied to each atom.

Proportional control schemes have been used that lead to frictional forces with values that depend on the difference between the desired temperature and the temperature of a given simulated system [10]. From the perspective of statistical mechanics, the most rigorous coupling scheme is that introduced by Nose' in which an integral control variable is introduced into the equations of motion [11,12]. This method, sometimes referred to as the Hoover-Nose' thermostat, not only produces a given average temperature, but also produces temperature fluctuations that are appropriate for a "sub-system" of atoms that is part of a

*Corresponding author. E-mail: brenner@ncsu.edu

Molecular Simulation
ISSN 0892-7022 print/ISSN 1029-0435 online © 2005 Taylor & Francis Group Ltd
http://www.tandf.co.uk/journals
DOI: 10.1080/08927020512331336898

macroscopic canonical ensemble [13]. This method is also time reversible, a feature missing from Langevin schemes that use random forces.

There are now available a large number of many-body analytic interatomic potential energy functions that are both sufficiently computationally efficient to be used in large-scale molecular simulations and that describe bonding properties with reasonable accuracy [14]. One of the most commonly used scheme for modeling metals is the embedded-atom method (EAM) that was introduced by Baskes, Daw and Foiles [15]. In this approach, which is based on effective medium theory [14], the electron density associated with a given atomic site is approximated by a superposition of electron densities contributed by neighboring atoms. The energy of an atom is taken as a function of this local electron density plus a pair-additive sum of interactions with neighboring atoms that mimic interatomic interactions between filled electron shells and between atomic nuclei. Electron densities are typically taken from electronic structure calculations (e.g. Hartree-Fock calculations), and an embedding function that relates the electron densities to the binding energy plus the pair-additive interactions are empirically fit to solid properties. These properties generally include the lattice constant, sublimation energy, elastic constants, phonon dispersion relations and thermal expansion coefficients. Other commonly used schemes, e.g. the Glue model [16] and the Finnis-Sinclair potential [17], are based on similar concepts.

The EAM and related many-body potentials have a proven ability to describe the structure, energy and the dynamics of a wide range of defects with reasonable accuracy. These structures include surfaces, steps, point defects, dislocations and stacking faults. The EAM can even provide a reasonably good description of liquid properties depending on the system. However, it is well established that the thermal transport properties of metals at room temperature are dominated by electronic degrees of freedom. Because explicit electronic degrees of freedom are replaced by an effective analytic interaction in schemes like the EAM, such schemes are unable to reproduce thermal transport properties at room temperature for metals no matter how accurately bonding and phonon properties are reproduced.

Recently Zhigilei and co-workers developed a multi-scale modeling scheme for treating the interaction of laser fields with metals [18–20]. In their approach the electronic and phonon contributions to the dynamics of the system are decoupled and treated using a combination of continuum and atomic dynamics. Interatomic forces were derived from EAM potentials, and continuum equations (including thermal transport equations) were solved step-wise on a grid superimposed over the atomic simulation.

In this paper, we analyze a simplification of the Zhigilei multiscale modeling approach that takes the form of an *ad hoc* thermostat that couples velocities in a MD simulation and a numerical solution of the continuum thermal transport equation. Our results demonstrate that coupling the continuum and atomic simulations via velocity scaling results in a non-physical "lag" between the kinetic energy profile of the simulation and the direct numerical solution of the continuum heat flow equation that results from the equipartitioning of the kinetic and potential energy in the simulation. On the other hand, it is shown that coupling the atomic and continuum equations via the Hoover thermostat equation (1) applied locally to each grid region produces kinetic energy profiles in the simulation that match the appropriate continuum result.

This continuum-atomistic thermostat scheme has several important advantages over other prior thermostating procedures. These advantages include the following: (1) experimental thermal transport properties can be incorporated into a simulation without explicitly including electronic degrees of freedom; (2) the temperature dependence of experimental thermal properties can be easily incorporated into the scheme; (3) in principle the effect of bulk defects such as dislocations and grain boundaries on heat transfer can be incorporated into the model by making appropriate changes in thermal properties around these defects; (4) the grid region can extend beyond the boundaries of an atomic simulation, coupling heat transport to macroscopic-scale boundary conditions; (5) numerical solutions of the continuum heat equations typically use step sizes comparable to those used in MD simulations for convenient grid spacings; and (6) the method is independent of the interatomic force model and is very straight forward to implement.

Details of the coupling scheme are given in the following section. Discussed in the subsequent two sections is a simulation of non-steady-state heat flow from a metal surface held at a constant temperature, and a simulation of a model tip moving along a silver surface. By doing the sliding simulations with and without the thermostating scheme, it is demonstrated that for large tip speeds the surface temperature and frictional force are strongly dependent on the thermal transport properties of the surface. A brief conclusion is given in the final section.

2. *Ad hoc* continuum-atomistic thermostat

In this thermostating scheme a MD simulation is divided into grid regions, and the temperature of each grid region is assigned according to the average kinetic energy of the atoms within that region (figure 1). New temperatures for each grid region are then calculated stepwise concurrent with the MD simulation by numerically solving the continuum heat equation

$$\frac{\partial T}{\partial t} = D\frac{\partial^2 T}{\partial R^2} \tag{2}$$

where T is the temperature derived from the MD simulation, and D is the thermal diffusivity given by

$$D = \frac{\lambda}{c_p \rho}. \tag{3}$$

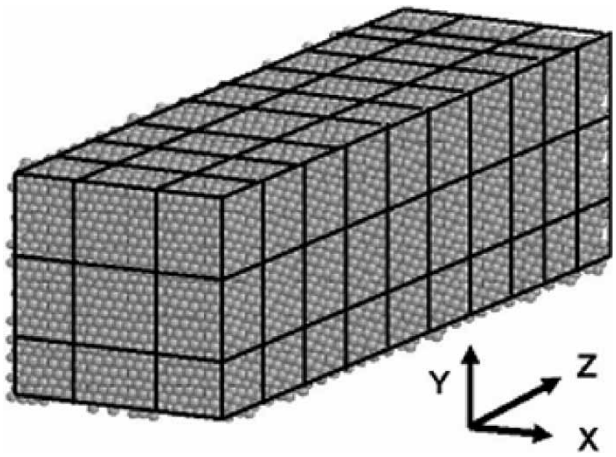

Figure 1. Illustration of the finite difference grid superimposed over an atomic simulation.

In equation (3), λ is the thermal conductivity, c_p is the heat capacity and ρ is the material density. The atomic velocities of the atoms in each grid region are scaled to match the solution of equation (2), and the atoms are then allowed to move according to the interatomic potential using the Hoover frictional force equation (1) applied locally to each grid region. This procedure produces a feedback between the kinetic energy of the simulation and the continuum heat transfer equation.

In the simplest implementation of this scheme, a Euler's method solution to equation (2), the temperature T^{new} for each grid region is given by

$$T^{\text{new}} = T^{\text{old}} + \Delta t\, D \frac{\partial^2 T}{\partial R^2} \tag{4}$$

where the partial derivative is calculated using a centered finite divided difference formula. For this scheme, the largest timestep $\Delta t^{\max}$ for numerical stability is given by

$$\Delta t^{\max} = \frac{1}{2D\left(\frac{1}{\Delta x^2} + \frac{1}{\Delta y^2} + \frac{1}{\Delta z^2}\right)} \tag{5}$$

where Δx, Δy and Δz are the grid spacings in the x, y and z directions, respectively. There are well known iterative numerical methods and better approximations for the temperature derivative that lead to stable numerical solutions for longer timesteps. However, the straightforward numerical scheme suggested here leads to timesteps that are comparable to those typically used in MD simulations (10^{-15} s), making other numerical methods largely unnecessary. For example, for gold at 300 K the experimental thermal diffusivity is 1.283×10^{-16} Å^2/s. With a uniform grid size of $\Delta x = \Delta y = \Delta z = 10$ Å the maximum time step size is about 1.2×10^{-15} s.

To incorporate temperature or defect dependent thermal properties, either the value used for D in equation (2) can depend on the temperature or defect density of a given grid region, or an explicit functional dependence of thermal properties on temperature can be included in the heat transport equation (2). For the examples discussed below we assume that thermal properties are temperature independent.

3. Simulated heat flow into bulk metals

To test the numerical stability of this coupled continuum-atomistic scheme, and to illustrate its application, a series of atomistic and continuum-atomistic MD simulations were carried out that model non-steady-state heat flow from a (111) surface kept at a constant temperature into the bulk of simulated silver, aluminum, nickel, copper and gold single crystals. The MD part of the simulation was carried out with EAM potentials using the *Paradyn* simulation code [21]. The system size was approximately $60 \times 60 \times 200$ Å for the x, y, and z dimensions, respectively, with periodic boundaries applied in the x and y directions. The number of atoms in each system varied between 47,000 and 66,000 atoms depending the material's lattice constant. The system for each metal was first equilibrated to 300 K for 5 ps using a Langevin thermostat and a time step size of 10^{-15} s. To create a temperature gradient the kinetic energy of the atoms within 10 Å of one end of the bar was maintained at 400 K by rescaling the atomic velocities at each time step using a Gaussian velocity distribution. This procedure produced heat flow along the $\langle 111 \rangle$ direction normal to the surface.

For the simulation using the continuum-atomistic thermostat, the simulation space was divided up into $6 \times 6 \times 20$ grid cells in the x, y and z directions, respectively, producing grid spacings of about 10 Å per side in each direction. The experimental values used for the thermal diffusivities for each metal are given in the table.

Plotted in the top panel of figure 2 as the squares is the average kinetic energy (reported as a temperature) as a function of depth from the surface for a MD simulation of EAM silver with the continuum-atomistic thermostat turned off. Data for two different times are shown. The solid lines in this plot correspond to the temperature profile from a numerical solution of the heat flow equation with no feedback from the MD simulation. The thermal diffusivity D for the numerical solution to the heat flow equation was determined by a least squares fit to the simulation data. The thermal diffusivity calculated using this method for each of the metals studied are given in the table along with the corresponding experimental values. As anticipated, the thermal diffusivities calculated from the atomistic simulations using strictly the EAM are much smaller than the experimental values.

Plotted in the middle panel of figure 2 are the simulated average atomic kinetic energy profiles for silver using the same conditions as those for the top panel except that the continuum-atomistic thermostat is turned on using the experimental thermal diffusivity. In this case the coupling is achieved by simply scaling the atomic velocities to match the temperature in each grid region as given by the numerical solution to the continuum heat equation.

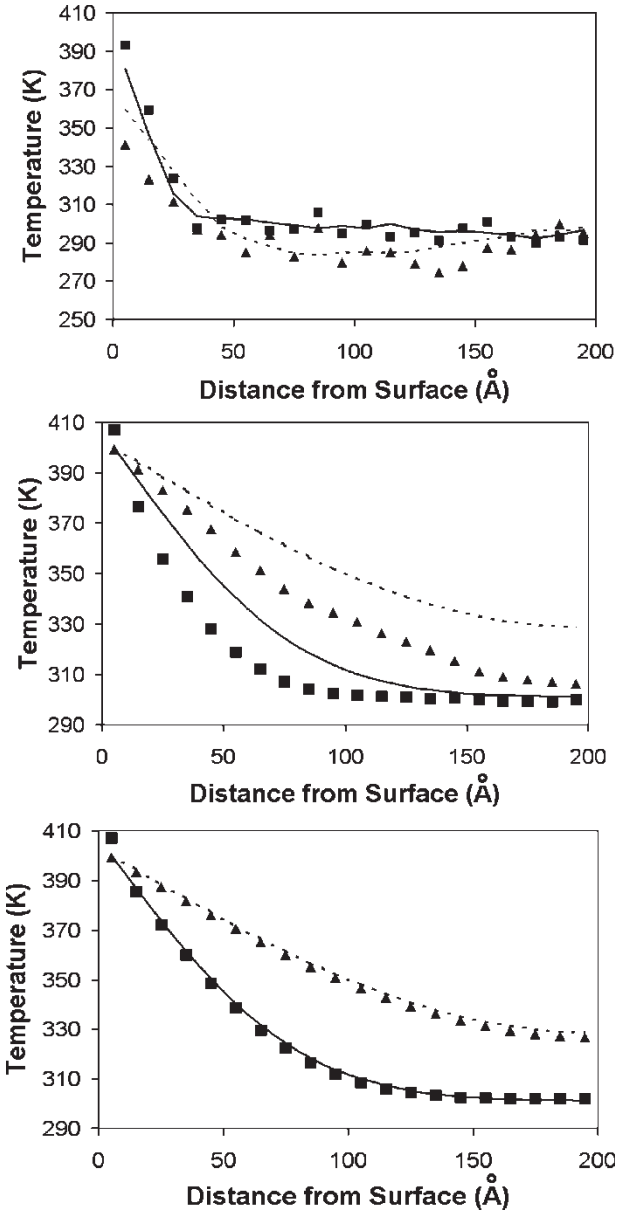

Figure 2. Kinetic energy (reported as a temperature) and temperature profiles for single crystal silver. The symbols are from the atomistic simulations; the lines are solutions to the continuum heat flow equation. *Top*: Heat flow from a silver (111) surface without the thermostat. The squares and solid line are for 1 ps and the triangles and dotted line are for 4 ps. The solid lines are a numerical solution to the heat flow equation with D fit to the simulation data. *Middle*: Using velocity scaling only in the simulation. The squares and solid line are for 0.1 ps; the triangles and the dotted line are for 0.5 ps. *Bottom*: Results using the Hoover thermostat. The symbols and lines are the same as for the middle panel.

The lines in the plot correspond to the temperature profile from a numerical solution of the heat flow equation using the same experimental value of thermal diffusivity but without feedback from the MD simulation. While the kinetic energy profile with the thermostat on matches more closely the expected profile from the continuum equations than the profile with the thermostat off, the profile "lags behind" the continuum solution calculated without feedback from the atoms. This result is because some of the kinetic energy after scaling the atomic velocities flows into potential energy as required by the equipartition of energy. Apparently when fed back into the numerical solutions of the continuum equation this slight transfer of kinetic energy is not sufficiently fast to keep up with heat flow, resulting in the "lag" of the temperature profile.

Table 1. Experimental and calculated (via the EAM) thermal diffusivities in units of Å^2/ps for various metals (experimental values are from [22])

Metal	*Experiment*	*EAM*
Silver	17,386	48
Aluminum	9786	144
Gold	12,737	18
Copper	11,625	124
Nickel	2295	174

Plotted in the bottom panel of figure 2 are data from the same simulation conditions as those used to generate the data in the middle panel except that a local Hoover frictional force equation (1) is applied to each atom. In this case the sum in equation (1) is over each atom in a given grid region, and therefore the friction coefficient is different for different grid regions. In this case the kinetic energy profile matches the analytic solution to the continuum heat flow equations very well. Essentially identical results, namely a profile lag with simple velocity scaling and excellent agreement with the continuum profile with the Hoover thermostat, were obtained for each of the metals listed in Table 1.

4. Model tip sliding across a gold substrate

As a second test case for the thermostat, the frictional force for a tip moving along a silver surface was calculated with and without the continuum-atomistic thermostat turned on. The simulated system is illustrated in figure 3. The system contains 300,000 atoms and has dimensions of 288 × 248 × 71 Å in the x, y and z directions. The system was oriented such that the z direction was normal to a (111) plane. Periodic boundaries where maintained in the x and y directions while the bottom surface was held rigid. The system was then divided into 29 × 25 × 7 grid regions. The tip is treated as a large single "atom" that

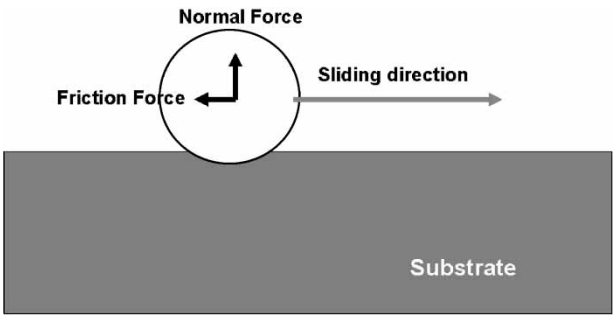

Figure 3. Illustration of the tip-surface simulation.

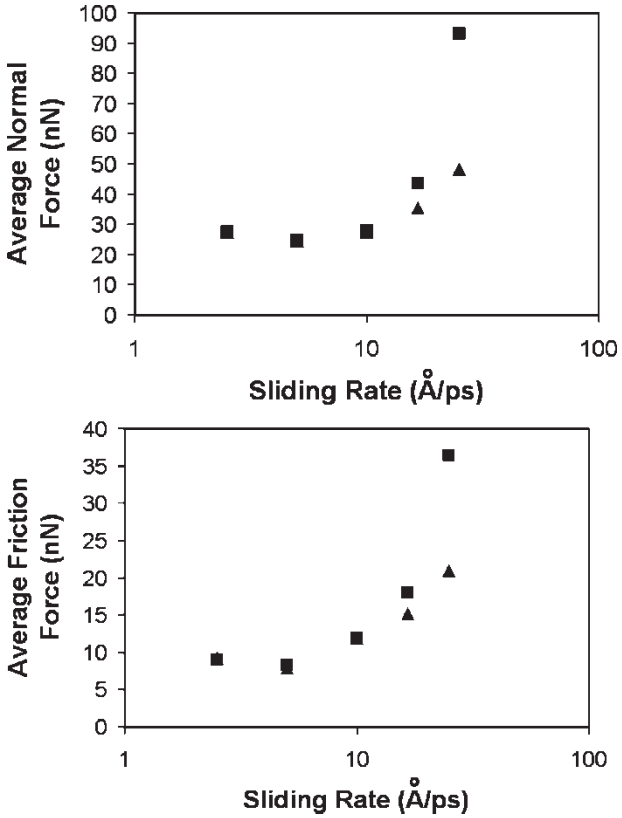

Figure 4. Average normal force (top) and frictional force (bottom) for a tip slid across a silver substrate as a function of sliding rate. The triangles and squares represent sliding with and without the thermostat applied, respectively.

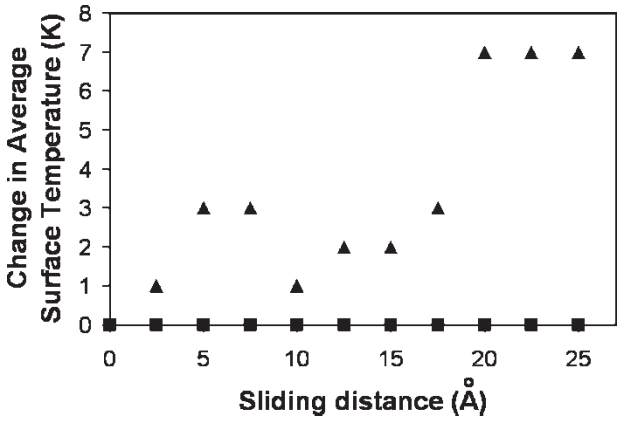

Figure 5. Change in the average surface temperature as a function of sliding distance for a tip sliding rate of 25 Å/ps. The triangles are for the system without the thermostat; the squares are for the system with the thermostat applied.

interacts with the atoms in the substrate via pair-additive repulsive forces. The force from the tip I on substrate atom i is given as

$$\begin{aligned} F_i &= 0 \qquad \text{for } r_{iI} \geq R \\ F_i &= -k(R - r_{iI})^n \quad \text{for } r_{iI} < R \end{aligned} \tag{6}$$

where R defines the radius of the spherical tip, r_{iI} is the radial distance from the center of the indenter to atom i, and n and k are constants related to the stiffness of the tip. For the substrate atoms the tip-atom forces are added to the EAM forces calculated using the Paradyn code. For convenience, values of $R = 40$ Å, $n = 1$ and $k = 1\,\text{eV/Å}^2$ were used for equation (6). The tip was indented to a depth of 2.5 Å and then was slid across a silver (111) surface along a (110) direction at different sliding speeds ranging between 2.5 and 25 Å/ps. The tip depth of 2.5 Å was chosen such that significant frictional forces were simulated but that no plastic damage occurred during the course of the simulation.

Plotted in figure 4 is the average normal and friction forces as a function of sliding rate for the simulation both with and without the continuum-atomistic thermostat (using the Hoover friction) applied to the system. Above sliding rates of approximately 10 Å/ps, the choice of thermostat has a very strong effect on the average normal and friction forces, with both the normal and frictional forces being higher with the thermostat. Plotted in figure 5 is the average surface temperature as a function of sliding distance for simulations with and without the thermostat for a sliding rate of 25 Å/ps. At the higher sliding rate there is appreciable heating of the surface without the thermostat, while with the thermostat turned on the heat is rapidly removed from the surface, and the surface temperature remains constant. As the temperature increases, the bonds are softened and the atoms are more easily pushed out of the way by the moving tip. This results in lower normal and friction forces. When the thermostat is applied the surface temperature does not increase as rapidly, which results in the higher normal and friction forces.

5. Conclusion

A new thermostat using an *ad hoc* coupling between numerical solutions of the continuum heat transport equations and a MD simulation has been characterized for two test cases, heat flow from a silver surface held at a constant elevated temperature, and a tip moving across a silver substrate. For the first case, we conclude that the thermostat procedure is numerically stable and can maintain kinetic energy profiles that match continuum temperature profiles using experimental thermal diffusivities provided that a Hoover frictional force is applied locally to each grid region. This thermostat therefore can significantly improve heat transport properties of simulated systems, especially for metals where the electronic degrees of freedom are responsible for the majority of heat transport at room temperature. For the case of the tip sliding across the silver substrate, non-physical heat buildup at the surface, at high sliding rates, is apparent in the simulations without the thermostat, and this heating can significantly influence friction and loading forces. With the thermostat applied, heat is more rapidly

dissipated from the surface, leading to greater friction and loading forces compared to the hotter surface.

The thermostat described here will have important uses for a number of applications, including simulations of high-speed sliding and machining. The thermostat is straight forward to implement and is independent of the potential function used in the simulations. One issue that has yet to be addressed is how latent heat associated with phase transitions can be incorporated into the formalism. We are currently exploring this and related issues, as well as exploring additional applications where this type of coupling could be valuable for molecular simulations.

Acknowledgements

This work was supported by the Office of Naval Research through grant N00014-04-2006.

References

[1] L.V. Woodcock. Isothermal molecular dynamics calculations for liquid salts. *Chem. Phys. Lett.*, **10**, 257 (1971).
[2] J.C. Tully. Dynamics of gas-surface interactions—3D Generalized Langevin Model applied to fcc and bcc surfaces. *J. Chem. Phys.*, **73**, 1975 (1980).
[3] S.A. Adelman. *Adv. Chem. Phys.*, **44**, 143 (1980).
[4] S.A. Adelman, J.D. Doll. Generalized Langevin equation approach for atom-solid-surface scattering—General formulation for classical scattering off harmonic solids. *J. Chem. Phys.*, **64**, 2375 (1976).
[5] M. Berkowitz, J.A. McCammon. Molecular-dynamics with stochastic boundaries. *Chem. Phys. Lett.*, **90**, 215 (1982).
[6] C.L. Brooks, M. Karplus. Deformable stochastic boundaries in molecular dynamics. *J. Chem. Phys.*, **79**, 6312 (1983).
[7] R.R. Lucchese, J.C. Tully. Trajectory studies of rainbow scattering from the reconstructured Si(100) surface. *Surf. Sci.*, **137**, 570 (1984).
[8] W.G. Hoover. *Molecular Dynamics*, Lecture Notes in Physics, Vol. 258, Springer-Verlag, Berlin (1986).
[9] D.J. Evans, W.G. Hoover, B.H. Failor, B. Moran, A.J.C. Ladd. Non-equilibrium molecular dynamics via Gauss principle of least constaint. *Phys. Rev. A*, **28**, 1016 (1983).
[10] H.J.C. Berendson, J.P.M. Postma, W.F. Vangunsteren, A. Dinola, J.R. Haak. Molecular dynamics with coupling to an external bath. *J. Chem. Phys.*, **81**, 3684 (1984).
[11] S. Nose'. A unified formulation of the constant temperature Molecular-Dynamics method. *J. Chem. Phys.*, **81**, 511 (1984).
[12] S. Nose'. A molecular dynamics method for simulations in the canonical ensemble. *Mol. Phys.*, **52**, 255 (1984).
[13] H.A. Posch, W.G. Hoover, F.J. Vesely. Canonical dynamics of the Nose' oscillator—Stability, order and chaos. *Phys. Rev. A*, **33**, 4253 (1986).
[14] D.W. Brenner, O.A. Shenderova, D.A. Areshkin. Quantum-based analytic interatomic forces and materials simulation. In *Reviews in Computational Chemistry*, K.B. Lipkowitz, D.B. Boyd (Eds), pp. 213–245, VCH Publishers, New York (1998).
[15] M.S. Daw, S.M. Foiles, M.I. Baskes. The Embedded-Atom method—A review of theory and applications. *Mat. Sci. Rep.*, **9**, 251 (1993).
[16] F. Ercolessi, M. Parrinello, E. Tosatti. Simulation of gold in the Glue model. *Phil. Mag. A*, **58**, 213 (1988).
[17] M.W. Finnis, J.E. Sinclair. A simple empirical N-Body potential for transition metals. *Phil. Mag. A*, **50**, 45 (1984).
[18] D.S. Ivanov, L.V. Zhigilei. Combined atomistic-continuum modeling of short-pulse laser melting and disintegration of metal films. *Phys. Rev. B*, **68**, 64114 (2003).
[19] D.S. Ivanov, L.V. Zhigilei. Effect of pressure relaxation on the mechanisms of short-pulse laser melting. *Phys. Rev. Lett.*, **91**(2003), 105701 (2003).
[20] L.V. Zhigilei, A.M. Dongare. Multiscale modeling of laser ablation: Applications to nanotechnology. *Comp. Modeling Eng. Sci.*, **3**, 539 (2002).
[21] S.J. Plimpton, B.A. Hendrickson. Parallel molecular dynamics with the Embedded Atom method. *Mat. Res. Soc. Symp. Proc.*, **291**, 37 (1993).
[22] CRC Handbook of Chemistry and Physics, 60th edition (CRC Press, Boca Raton, 1980).